SCIENTIFIC REPORTS

OPEN

SUBJECT AREAS:
CELLULAR NEUROSCIENCE
BRAIN
MOLECULAR NEUROSCIENCE

Received
27 June 2014

Accepted
26 August 2014

Published
15 September 2014

Correspondence and requests for materials should be addressed to M.S. (makosato@anat2.med.osaka-u.ac.jp)

Filamin A-interacting protein (FILIP) is a region-specific modulator of myosin 2b and controls spine morphology and NMDA receptor accumulation

Hideshi Yagi[1,2,3], Takashi Nagano[1], Min-Jue Xie[1,2], Hiroshi Ikeda[2,4], Kazuki Kuroda[1,2], Munekazu Komada[1,2], Tokuichi Iguchi[1,2,9], Rahman M. Tariqur[1], Soichi Morikubo[1,5], Koichi Noguchi[3], Kazuyuki Murase[2,4], Masaru Okabe[6] & Makoto Sato[1,2,7,8,9]

[1]Division of Cell Biology and Neuroscience, Department of Morphological and Physiological Sciences, Faculty of Medical Sciences, University of Fukui, Fukui 910-1193, Japan, [2]Research and Education Program for Life Science, University of Fukui, Fukui 910-8507, Japan, [3]Department of Anatomy and Neuroscience, Hyogo College of Medicine, Hyogo 663-8501, Japan, [4]Department of Human and Artificial Intelligence Systems, Faculty of Engineering, University of Fukui, Fukui 910-8507, Japan, [5]Division of Ophthalmology, Department of Sensory and Locomotor Medicine, Faculty of Medical Sciences, University of Fukui, Fukui 910-1193, Japan, [6]Department of Experimental Genome Research, Genome Information Research Center, Osaka University, Osaka 565-0871, Japan, [7]Research Center for Child Mental Development, University of Fukui, Fukui 910-1193, Japan, [8]United Graduate School of Child Development, Osaka University, Kanazawa University, Hamamatsu University School of Medicine, Chiba University and University of Fukui, Osaka 565-0871, Japan, [9]Department of Anatomy and Neuroscience, Graduate School of Medicine, Osaka University, Osaka 565-0871, Japan.

Learning and memory depend on morphological and functional changes to neural spines. Non-muscle myosin 2b regulates actin dynamics downstream of long-term potentiation induction. However, the mechanism by which myosin 2b is regulated in the spine has not been fully elucidated. Here, we show that filamin A-interacting protein (FILIP) is involved in the control of neural spine morphology and is limitedly expressed in the brain. FILIP bound near the ATPase domain of non-muscle myosin heavy chain IIb, an essential component of myosin 2b, and modified the function of myosin 2b by interfering with its actin-binding activity. In addition, FILIP altered the subcellular distribution of myosin 2b in spines. Moreover, subunits of the NMDA receptor were differently distributed in FILIP-expressing neurons, and excitation propagation was altered in *FILIP*-knockout mice. These results indicate that FILIP is a novel, region-specific modulator of myosin 2b.

Filamentous actins (F-actins) are important structural components that, together with a variety of actin-binding proteins, underlie a broad range of cellular responses. For example, F-actins and their binding partners play pivotal roles in cell motility and directionality at the leading edge of migrating cells[1]. In addition, actin-binding proteins dynamically regulate the structure of neural spines, which are actin-rich protrusions on neurons and major sites for excitatory synaptic transmission involved in learning and memory[2,3]. To date, more than 100 actin-binding proteins have been identified; muscle-type myosin and filamin were among the first such proteins to be characterised, whereas non-muscle myosins, including myosin 2b, are emerging members of this group and have attracted much attention because of their essential involvement in diverse fundamental cellular functions, spine structure dynamics and learning and memory[4,5,6,7]. Although there is much interest in the mechanisms of actin-binding protein regulation, which is critical for essential cellular functions, these mechanisms have not yet been fully elucidated. We previously identified a novel filamin A binding protein, filamin A-interacting protein (FILIP or FILIP-1), and demonstrated that FILIP participates in actin dynamics by accelerating the calpain-dependent degradation of filamin A[8], which, when mutated, causes human migration disorder[9,10]. We have demonstrated that FILIP, whose mRNA is localised in the ventricular zone of the cortex during the perinatal stage, is potentially involved in radial migration in the cortex by introducing exogenous FILIP into the ventricular zone[8]. However, the *in vivo* role of FILIP, especially in adults, has not yet been clarified. Here, we

generated a *FILIP*-knockout mouse to address these issues. Unexpectedly, we found that FILIP is likely to regulate spine structure by modulating the activity of myosin 2b.

Learning and memory are dependent on the activity and morphology of the neural spines[11]. Morphological changes to a spine depend on actin dynamics[12]. In the hippocampus, myosin 2b is a key regulator of the changes in spine morphology related to learning and memory[4,6]. However, how and why neural spine morphology varies across the cortex remains unknown, especially in response to learning. During the learning response, spine enlargement is observed during long-term potentiation (LTP) in the hippocampus[11], whereas learning induces a reduction in the volume of the spine head in the piriform cortex[13]. Although the mechanisms underlying such differences have not been fully elucidated, our data suggest that FILIP, which is expressed in the piriform cortex but not in the hippocampus, is one of the molecules responsible for these differences.

Results

Generation of a *FILIP*-knockout mouse. To investigate the function of FILIP, *FILIP* was disrupted through homologous recombination. In embryonic stem cells, a 2.8-kb genomic fragment containing a portion of exon 5 (the largest exon of *FILIP*) was replaced with in-frame *β-galactosidase* and *neomycin resistance* genes (see Supplemental Fig. S1a online). The chimeras were backcrossed with C57BL/6 mice to produce *FILIP*-heterozygous mice. The appearance of and histological samples from the *FILIP*-heterozygous ($FILIP^{+/-}$) mice were indistinguishable from those of their wild-type ($FILIP^{+/+}$) littermates. The homozygous ($FILIP^{-/-}$) mice were indistinguishable from their normal littermates in terms of appearance. The disruption of the *FILIP* gene and absence of FILIP protein were confirmed by northern blot and western blot analyses (see Supplemental Fig. S1b, c online). Although two alternatively spliced forms of FILIP, a long form (L-FILIP) and a short form (S-FILIP), were observed in the rat, only one form, corresponding to the long form of FILIP, was detected in mice. Hereafter, we refer to this form as FILIP instead of L-FILIP.

Targeting of FILIP revealed limited localisation of FILIP in the brain. Because the mutant allele conferred β-galactosidase expression under the control of the *FILIP* promoter (see Supplemental Fig. S1d online), we examined the distribution of FILIP-expressing cells in the adult mouse brain by visualising β-galactosidase activity. With the exception of modestly accumulated neurons in the upper cortical layer of the $FILIP^{+/-}$ mice, no obvious difference was observed in terms of the distribution between $FILIP^{+/-}$ and $FILIP^{-/-}$ mice (see Supplemental Fig. S2a–f online).

Many β-galactosidase-positive cells were detected in the forebrain, particularly in the ventral portion and in the deep nuclei (Fig. 1 and Supplemental Fig. S2a–f online), including the anterior olfactory nucleus, the piriform cortex and the olfactory tubercle as well as in the nucleus accumbens, the globus pallidus and the amygdaloid complex. In addition, positive cells were observed in the neocortex, especially in the visual and the motor cortices (Fig. 1). In contrast, β-galactosidase-positive cells were rarely observed in the hippocampus. In the diencephalon, β-galactosidase activity was faint, except in cells in the arcuate nucleus (Fig. 1f and Supplemental Fig. S2c online).

FILIP is expressed in glutamatergic neurons. β-galactosidase-positive cells were positive for the neuronal markers NeuN and MAP-2 (see Supplemental Fig. S2g online)[14,15] and for Brn1, which is expressed principally in neurons of layers II–V[16], the visual cortex and the piriform cortex (see Supplemental Fig. S2h online). We further investigated the types of neurons that express FILIP. FILIP containing neurons were not positive for GAD67 in the piriform cortex (see Supplemental Fig. S2g online), indicating that FILIP is expressed in glutamatergic neurons but not in GABAergic neurons.

FILIP regulates spine length. We next investigated whether FILIP controls neuronal morphology. Neurons were visualised using the Golgi-Cox staining method, and the lengths of the spines (the distance between the spine neck close to the dendrite and the tip; Fig. 2a) on the apical dendrites of the layer II pyramidal neurons (superficial pyramidal neurons) in the piriform cortex were measured. The mean length of the spines was shorter in $FILIP^{-/-}$ mice (mean ± s.d., 1.00 ± 0.16 μm; n = 15) than in the control $FILIP^{+/-}$ and $FILIP^{+/+}$ littermates (1.17 ± 0.16 μm; n = 19; Fig. 2b–c; Student's *t*-test, two-tailed, p = 0.00358). The proportion of the stubby, mushroom and thin types of spines is indicative of spine maturation[17,18]. The measured differences of spine types did not achieve significance (Fig. 2d). Then, we constructed an inducible knockdown vector for *FILIP* and transfected the piriform neurons with this vector (Fig. 2e). We found that the mean spine length of *FILIP*-knockdown neurons was shorter (0.95 ± 0.09 μm; n = 20) than that of control neurons (1.06 ± 0.06 μm; n = 12; Fig. 2f–g; Student's *t*-test, two-tailed, p = 0.00059). We then studied the influence of *FILIP* knockdown on the spine morphology with primary cultured piriform neurons (Fig. 2h). We observed that the mean spine length of *FILIP*-knockdown neurons (1.29 ± 0.84 μm; 398 spines in 5 neurons) was significantly shorter than that of control neurons (1.53 ± 0.91 μm; 432 spines in 5 neurons; Fig. 2i; Student's *t*-test, two-tailed, p = 0.00011). We also found that the estimated spine volume of *FILIP*-knockdown neurons (0.33 ± 0.41 μm^3; 241 spines in 5 neurons) was significantly larger than that of control neurons (0.22 ± 0.24 μm^3; 326 spines in 5 neurons; Fig. 2j; Wilcoxon rank sum test, p = 0.00015).

FILIP was not expressed in pyramidal neurons in the hippocampus (Fig. 1f–h and Supplemental Fig. S2c–e online). Therefore, these hippocampal neurons can be used as an ideal system to study the role of FILIP through ectopic expression studies. Hippocampal neurons were taken from E17.5 mice, cultured for 20 days in vitro (DIV20) and transfected with an expression vector for Asp-Tyr-Lys-Asp-Asp-Asp-Asp-Lys (FLAG)-tagged FILIP (FILIP-FLAG). Two days after transfection, we examined the localisation of exogenous FILIP based on FLAG staining. FILIP was identified in the spines as well as in dendrites (Fig. 3a). We further investigated whether the ectopic expression of FILIP influences spine morphology. We transfected the FILIP expression vector into hippocampal neurons at DIV17; 3 days later, we measured the spine length and volume (Fig. 3b–e). The mean spine length in the neurons with FILIP was longer (0.97 ± 0.40 μm; 912 spines in 13 neurons) than in those without exogenous FILIP (0.87 ± 0.38 μm; 843 spines in 12 neurons; Fig. 3d; Student's *t*-test, two-tailed, p < 0.00001). The spine head volume was reduced compared with spines without FILIP (0.19 ± 0.20 μm^3; 433 spines from 11 FILIP-expressing neurons and 0.27 ± 0.27 μm^3; 397 spines from 11 control neurons; Fig. 3e; Wilcoxon rank sum test, p < 0.00001).

FILIP binds to non-muscle myosin heavy chain IIb. Although FILIP binds to filamin A and is involved in controlling filamin A degradation[8], filamin A expression decreased in the postnatal telencephalon despite its high expression during the embryonic period (Fig. 4a). Recently, it has been reported that small amounts of filamin A are expressed in the dendrites and cell soma but not spines of adult neurons[19]. Therefore, we examined how FILIP exerts its function in the absence of filamin A in the spine. We determined that non-muscle myosin heavy chain IIb (NMHC IIb) is a novel FILIP-binding partner. In general, non-muscle myosin is composed of 2 heavy chains and 4 light chains[20]. NMHC IIb is a heavy chain of myosin 2b and is essential for the actin-binding and ATPase activity of myosin 2b[5]. FILIP-FLAG and NMHC IIb in COS-7 cells were successfully co-immunoprecipitated using an anti-NMHC IIb antibody (Fig. 4b). The NMHC IIb binding sites on FILIP were investigated using several fragments of FILIP (Fig. 4c,

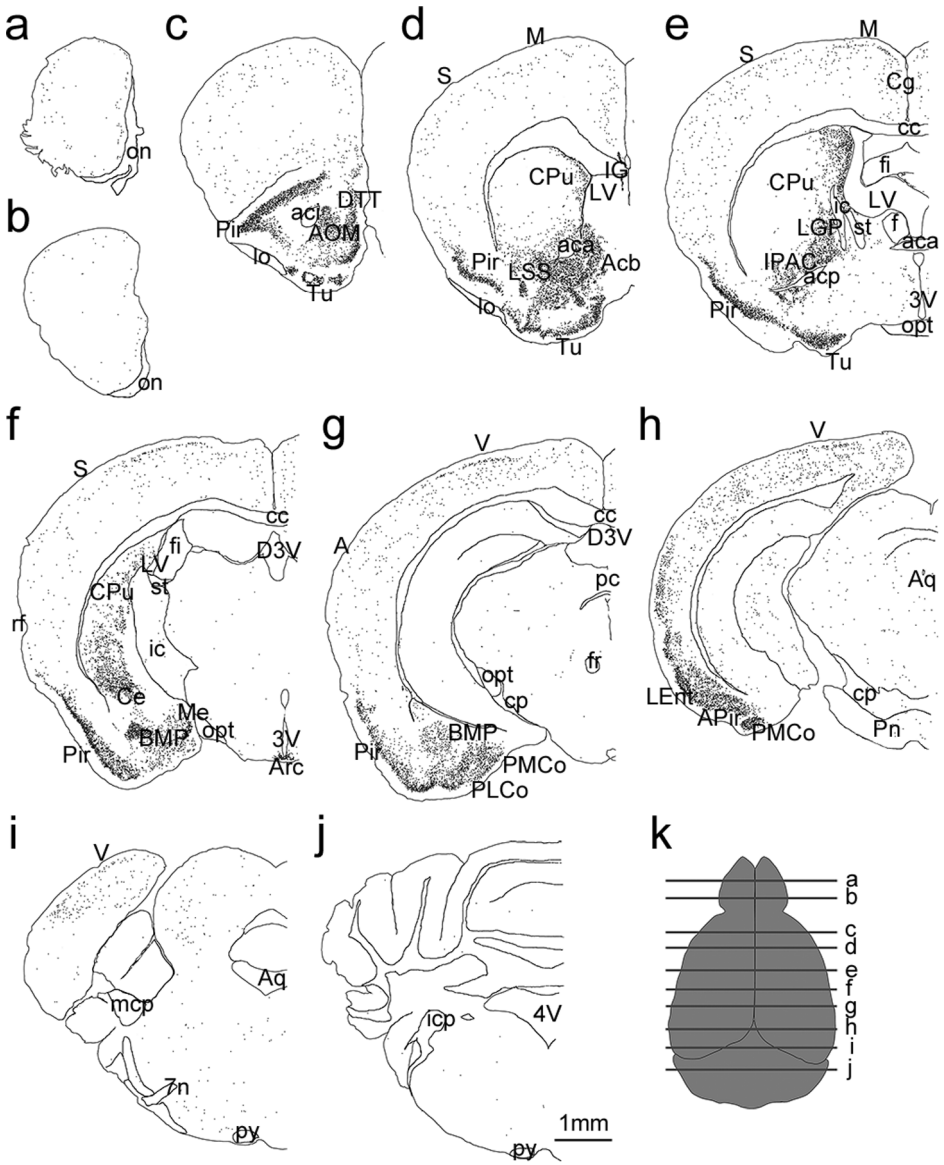

Figure 1 | Localisation of FILIP-positive cells in the adult brain. The cells positive for β-galactosidase staining (expressed under the control of the *FILIP* promoter) are represented by black dots. The coronal sections of an adult (12 week-old) *FILIP*$^{-/-}$ mouse brain are shown. The positions of coronal sections (a) to (j) are shown in (k). The abbreviations are as follows. A, auditory cortex; aca, anterior commissure, anterior part; Acb, nucleus accumbens; aci, anterior commissure, intrabulbar part; acp, anterior commissure, posterior; AOM, anterior olfactory nucleus, medial part; APir, amygdalopiriform transition area; Aq, aqueduct; Arc, arcuate nucleus; BMP, basomedial amygdaloid nucleus, posterior part; cc, corpus callosum; Ce, central amygdaloid nucleus; Cg, cingulate cortex; cp, cerebral peduncle, basal part; CPu, caudate putamen; DTT, dorsal tenia tecta; D3V, dorsal third ventricle; f, fornix; fi, fimbria of the hippocampus; fr, fasciculus retroflexus; ic, internal capsule; icp, inferior cerebellar peduncle; IG, indusium griseum; IPAC, interstitial nucleus of the posterior limb of the anterior commissure; LEnt, lateral entorhinal cortex; LGP, lateral globus pallidus; lo, lateral olfactory tract; LSS, lateral stripe of the striatum; LV, lateral ventricle; M, motor cortex; mcp, middle cerebellar peduncle; Me, medial amygdaloid nucleus; on, olfactory nerve layer; opt, optic tract; pc, posterior commissure; Pir, piriform cortex; PLCo, posterolateral cortical amygdaloid nucleus; PMCo, posteromedial cortical amygdaloid nucleus; Pn, pontine nuclei; py, pyramidal tract; rf, rhinal fissure; S, somatosensory cortex; st, stria terminalis; Tu, olfactory tubercle; V, visual cortex; 3 V, third ventricle; 4 V, fourth ventricle and 7 n, facial nerve.

d). The fragment containing amino acids (aa) 1–652 of FILIP did not co-immunoprecipitate with NMHC IIb; however, the 687–1212 aa fragment of FILIP did co-immunoprecipitate with NMHC IIb (Fig. 4d). Therefore, the NMHC IIb binding site was assigned to the C-terminal region between 687–1212 aa of FILIP. Because the 960–1212 aa fragment of FILIP did not co-immunoprecipitate with NMHC IIb (Fig. 4d), the 687–960 aa region of FILIP is likely to be important for binding to NMHC IIb. Conversely, FILIP-FLAG co-immunoprecipitated with the 1–782 aa and 1–331 aa regions of NMHC IIb but not with the 90–331 aa region (Fig. 4e–g). The myosin heavy chain has a globular head domain that is critical for the contractive activity of myosin 2b. Biochemically, the globular head domain of NMHC IIb consists of the myosin N-terminal, the upper 50 kDa, the lower 50 kDa and the converter subdomain; crystal structure analyses indicate that ATP binds in a pocket between the upper 50 kDa and the N-terminal subdomain located within the 1–90 aa region of NMHC IIb[20]. Our data indicate that FILIP binds to the globular head domain near the ATP binding site that controls the conformational change of NMHC IIb and is needed for the contractile cycle, which consists of dissociation and binding to F-actins.

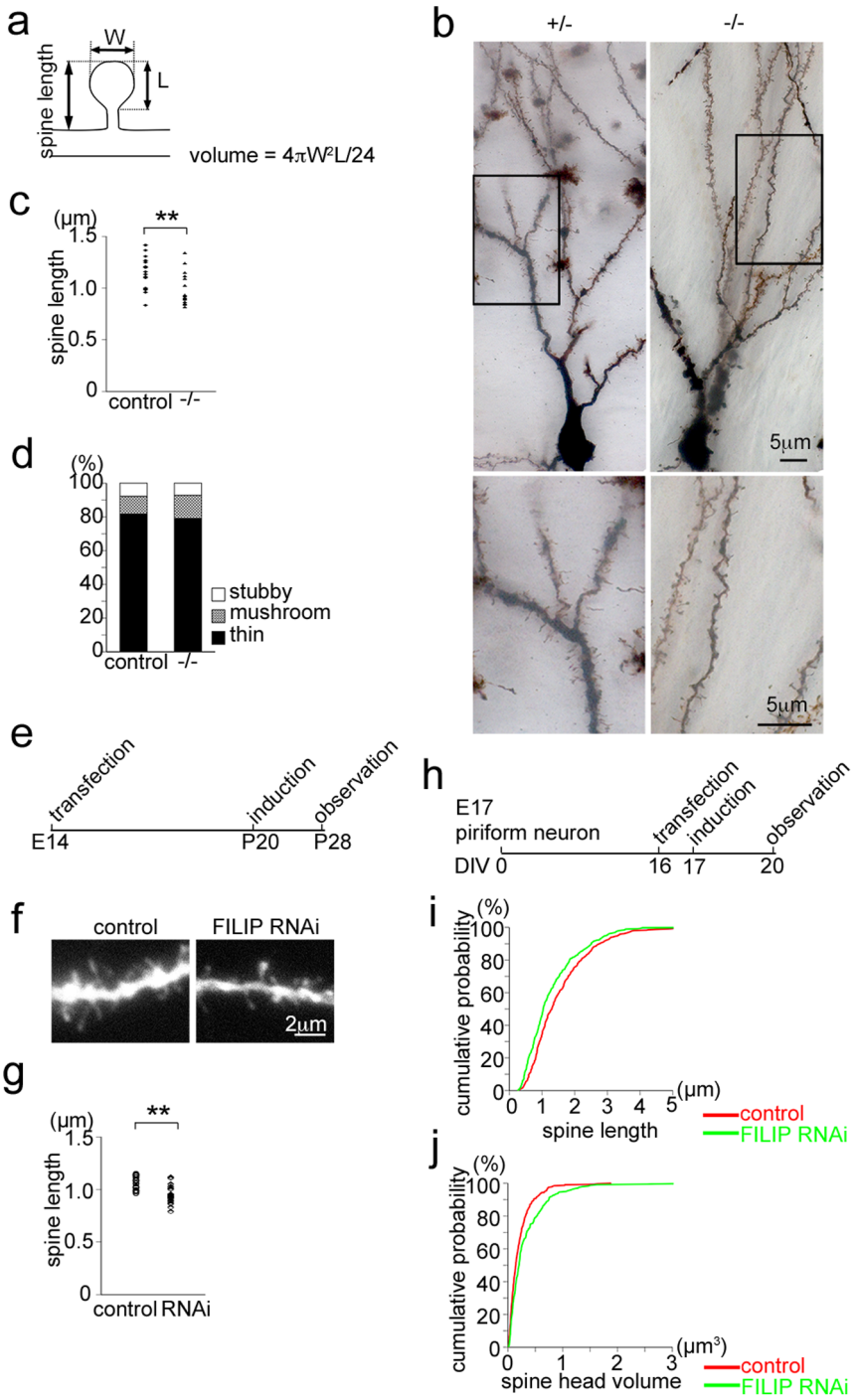

Figure 2 | FILIP controls spine shape in the piriform cortex. (a) A schematic of the spine indicates the locations where the measurements were performed. The spine head volume was calculated from the width (W) and length (L) of the spine head under the assumption that the spine is a spheroid. (b) The morphology of layer II pyramidal neurons located in the piriform cortex. High magnification images of the boxed area are shown in the bottom row. (c) There was a significant difference in the mean spine length of the layer II piriform pyramidal neurons between 4 *FILIP*$^{-/-}$ mice and 4 *FILIP*$^{+/-}$ and *FILIP*$^{+/+}$ littermates. **p = 0.00358 (Student's *t*-test). (d) FILIP was not apparently involved in spine classification. (e) The experimental schedule for panels (f) and (g) is shown. (f) The inducible knockdown of FILIP in the piriform cortex resulted in shorter spine length. (g) There was a significant difference in the mean spine length between the control and knockdown neurons located in the piriform cortex; ** p = 0.00059. (h) The experimental schedule for panels (i) and (j) is shown. (i) The cumulative probability of the spine length is shown. (j) The cumulative probability of the spine head volume is shown.

FILIP influences the subcellular distribution of myosin 2b. Because FILIP binds to the head domain of NMHC IIb, which is essential for the binding of NMHC IIb to actin fibres, it is likely that FILIP modifies the ability of myosin 2b to bind to F-actins. First, we determined how FILIP is involved in the interaction of myosin 2b with F-actins using COS-7 cells. Because F-actin is capable of forming stress fibres in COS-7 cells, the use of COS-7 cells allowed us to investigate the influence of FILIP on the interaction of myosin 2b with F-actin. In terms of myosin 2b distribution, we classified cells into the following two categories:

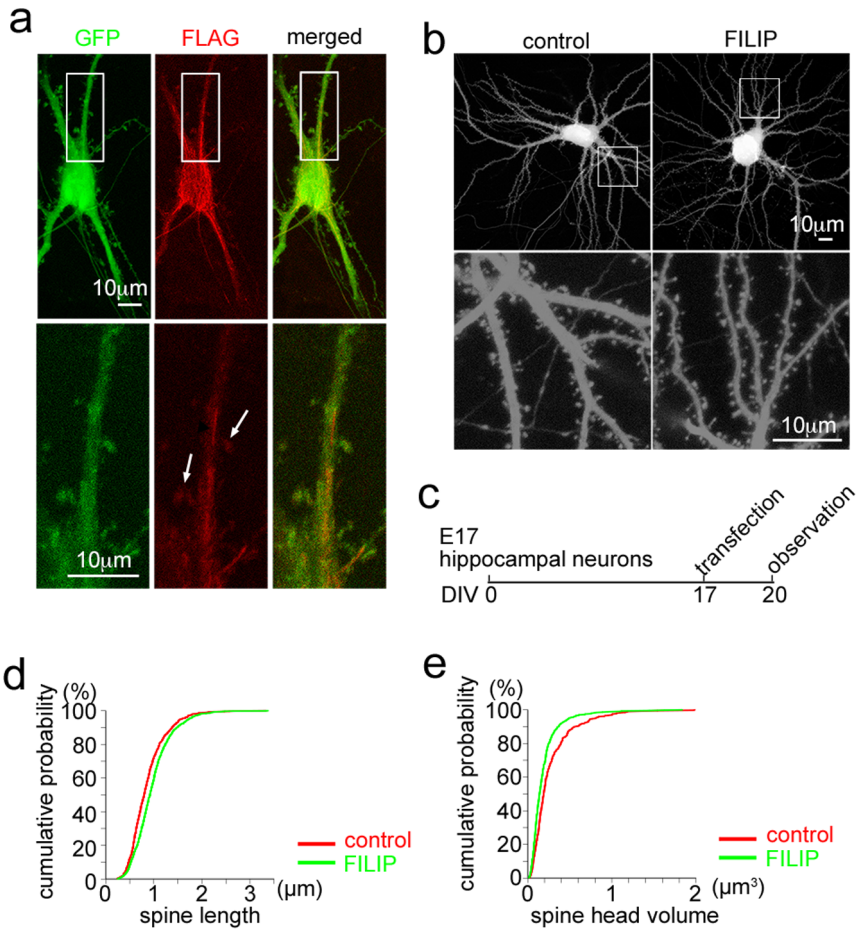

Figure 3 | Exogenous FILIP modifies the spine shape of the hippocampal neurons. (a) Exogenous FILIP localised to dendritic spines and dendrites of primary cultured hippocampal neurons. High-magnification images of the boxed area are shown in the bottom row. Arrows indicate FILIP based on FLAG staining in spines. (b) Exogenous FILIP influenced the morphology of primary cultured hippocampal neurons. High-magnification images of the boxed area are shown in the bottom row. (c) The experimental schedule for panels (b), (d) and (e) is shown. (d) The cumulative probability of the spine length is shown. (e) The cumulative probability of the spine head volume is shown. The spine head volume was significantly reduced in FILIP-expressing neurons.

cells with stress fibre-like distribution and cells with granular distribution. "Stress fibre-like distribution" indicates that the cells have thick and long fibre-like structures of NMHC IIb, and "granular distribution" indicates that NMHC IIb exhibits a particle-like localisation without thick fibre-like structures. Whereas the stress fibre-like distribution of myosin 2b was dominant in COS-7 cells without endogenous FILIP, the number of cells with granular myosin 2b distribution surpassed that of cells with stress fibre-like distribution in the presence of FILIP (see Supplemental Fig. S3a, b online). We next investigated whether FILIP influenced the formation of actin stress fibres, as myosin 2 is a component of actin stress fibres[21,22]. The number of cells with actin stress fibres decreased in the presence of FILIP (see Supplemental Fig. S3c, d online). Because FILIP binds to the N-terminal domain of myosin 2b, which is essential for binding to actin fibres, and the binding of myosin 2b to actin fibres is essential for the function of myosin 2b, we hypothesised that FILIP interferes with the activity of myosin 2b. We then compared the appearance of NMHC IIb in COS-7 cells in the presence of the myosin 2b inhibitor blebbistatin. Blebbistatin binds to the myosin globular head domain and blocks the rigid binding of myosin 2b to actin[23]. A similar "granular distribution" of NMHC IIb was observed in the presence of blebbistatin (see Supplemental Fig. S3e, f online).

FILIP interferes with the binding of myosin 2b to F-actins. If our hypothesis that FILIP interferes with myosin 2b binding to F-actins is correct, the amount of myosin 2b associated with F-actins should decrease in the presence of FILIP. F-actins exist in equilibrium with free globular (G)-actins. Because actins in the cytosol can be fractionated into F-actin-rich (Triton-soluble (TS) fraction in Supplemental Fig. S4a online) and G-actin-rich fraction (cytosolic (CS) fractions in Supplemental Fig. S4a online), we examined the amounts of NMHC IIb in these two fractions. We found that the amount of NMHC IIb in the G-actin-rich fraction (free NMHC IIb) increased in the presence of FILIP, whereas the amount of NMHC IIb in the F-actin-rich fraction decreased (see Supplemental Fig. S4b online), suggesting that less NMHC IIb is associated with F-actins in the presence of FILIP. These results indicated that FILIP controlled the binding of myosin 2b to F-actin. As FILIP controls the degradation of filamin A, we investigated whether the amount of myosin 2b was also influenced by FILIP expression in our culture conditions. We found that the total amounts of myosin 2b and filamin A did not change much after FILIP expression in some culture cells (see Supplemental Fig. S5a online). However, we found that the amount of NMHC IIb increased by approximately 40% in the hearts of *FILIP*$^{-/-}$ mice (see Supplemental Fig. S5b online), suggesting that deletion of FILIP increased the amount of NMHC IIb. We also found that the mean intensity of immunostaining of myosin 2b was significantly increased in the primary cultured piriform neurons of the *FILIP*$^{-/-}$ mice (187.5 ± 23.6; 44 neurons) compared with that of the control mice (149.8 ±

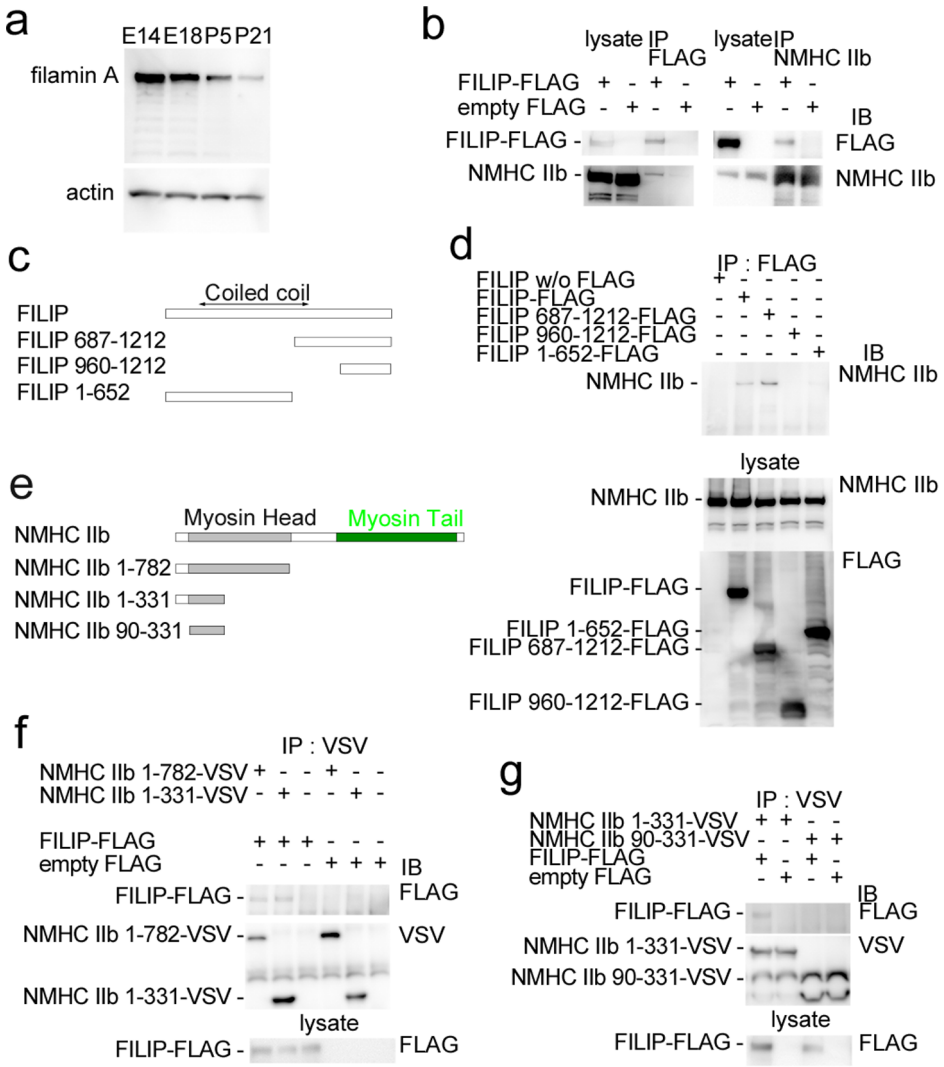

Figure 4 | FILIP binds to non-muscle myosin heavy chain IIb (NMHC IIb) of myosin 2b. (a) Filamin A expression in the telencephalon decreased as development advanced. (b) FILIP bound to endogenous NMHC IIb. The lysates of COS-7 cells transfected with a FLAG-tagged FILIP expression vector or an empty vector were immunoprecipitated using anti-FLAG and anti-NMHC IIb antibodies. Co-immunoprecipitation of FILIP and NMHC IIb was verified using anti-FLAG and anti-NMHC IIb antibodies to detect FILIP and NMHC IIb, respectively. (c) The wild-type and mutant forms of FILIP used in this study are shown. The arrowed line indicates the coiled-coil region. (d) FILIP bound to NMHC IIb via the C-terminal half of FILIP. FLAG-tagged full-length FILIP and FILIP 687–1212 co-immunoprecipitated with endogenous NMHC IIb. (e) The NMHC IIb and mutated NMHC IIb used in this study are shown. The grey box indicates the myosin head domain. The green box indicates the myosin tail domain. (f) NMHC IIb bound to FILIP via the N-terminal half of the myosin head domain. FLAG-tagged FILIP co-immunoprecipitated with NMHC IIb 1-782-VSV and NMHC IIb 1-331-VSV. (g) The myosin N-terminal SH3-like domain of NMHC IIb was responsible for binding to FILIP. FLAG-tagged FILIP co-immunoprecipitated with VSV-tagged NMHC IIb 1-331, whereas FLAG-tagged FILIP did not co-immunoprecipitate with VSV-tagged NMHC IIb 90-331.

32.0; 44 neurons; Welch's *t*-test, two-tailed, $p < 0.00001$; see Supplemental Fig. S5c online). This change in the intensity of NMHC IIb in FILIP-expressing neurons was also observed in the *FILIP*$^{+/-}$ piriform cortex (see Supplemental Fig. S5d online).

FILIP influences the subcellular distribution of myosin 2b in spines. It has been demonstrated that myosin 2b localises to the lower part of the spine head and the spine neck[7,24] and that the inhibition of myosin 2b leads to spine elongation and reduced spine head volume[4,7]. We performed *myosin 2b* knockdown and obtained similar results (see Supplemental Fig. S6 online). Therefore, it is likely that FILIP modulates spine morphology through myosin 2b. We then investigated whether the subcellular localisation of NMHC IIb was altered in spines in the presence or absence of FILIP. We transfected morphologically pyramidal neurons that had been isolated and cultured from the piriform cortices of the *FILIP*$^{-/-}$ mice and those of the control littermates with tdTomato as a volume marker and an EGFP-tagged NMHC IIb and analysed the subcellular distribution of exogenous NMHC IIb. The subcellular distribution of NMHC IIb correlated well with the tdTomato signals in the spine of control mice but not in that of the *FILIP*$^{-/-}$ mice (Fig. 5a–c). We also investigated the distribution of internal NMHC IIb in the piriform cortex neurons taken from *FILIP*$^{-/-}$ mice and found that the number of spines with accumulated signals of NMHC IIb increased in the neurons from the *FILIP*$^{-/-}$ mice (Fig. 5d, e). These results indicate that FILIP altered the subcellular distribution of myosin 2b from its proximally accumulated pattern to an ubiquitous localisation.

Overexpression of NMHC IIb inhibits the spine elongation induced by exogenous FILIP expression. We observed that exogenous FILIP influenced endogenous NMHC IIb distribution in the spine of

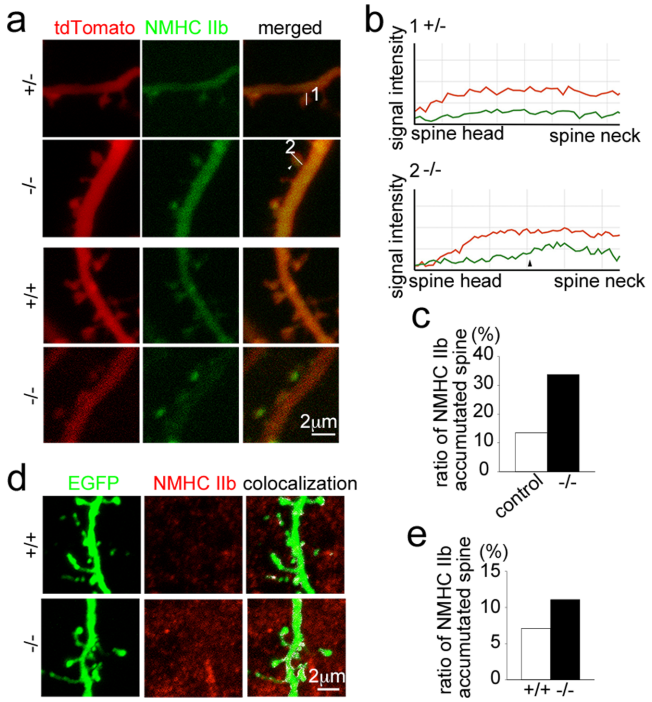

Figure 5 | FILIP modulates the subcellular distribution of NMHC IIb in the pyramidal neurons of the piriform cortex. (a) NMHC IIb distributed diffusely in the spine heads of piriform cortex neurons of control mice (+/−, +/+). In the absence of FILIP (−/−), NMHC IIb localized to the neck region of spines. The middle panels show the distribution of EGFP-tagged NMHC IIb, and the left panels show the morphology of the spines detected using the tdTomato signal. (b) The line profile was measured along the white lines shown in the right panels of (a). The red and green lines represent the intensities of tdTomato and EGFP, respectively. The white arrowhead shown in the right panels of (a), and the black arrowhead shown in 2 indicate positions where the signal intensity of EGFP was increased compared with tdTomato. (c) An accumulation of the exogenous NMHC IIb in the spine was more often observed in the piriform cortical neurons derived form the *FILIP*$^{-/-}$ mice than those of the control mice (data obtained from 126 spines of the control neurons and 95 spines of the *FILIP*$^{-/-}$ neurons; p = 0.00052, Fisher's exact test, two-tailed). (d) An accumulation of endogenous NMHC IIb was more often observed in the spines of the piriform cortex neurons derived from the *FILIP*$^{-/-}$ mice than those from the wild-type mice. In the right column, the area where the NMHC IIb and EGFP signals colocalised is highlighted in white. (e) The summarised data of 579 spines (control) and 777 spines (the *FILIP*$^{-/-}$ mice) are shown (p = 0.0141, Fisher's exact test, two-tailed).

hippocampal neurons (Fig. 6a, b). If we assume that exogenous FILIP elongated the spine through binding to myosin 2b and interfering with its function, then exogenous NMHC IIb should be able to rescue the influence of FILIP on spine morphology. We transfected the FILIP expression vector and NMHC IIb expression vector into primary cultured hippocampal neurons and examined spine length. We found that the exogenous expression of NMHC IIb inhibited the spine elongation caused by exogenous FILIP (Fig. 6c, d).

FILIP intermingles with NMDA receptor-mediated signalling. Experimentally, glycine is applied to neurons to enhance the activation of NMDA receptors[25,26]. We therefore investigated whether FILIP influences spine morphology in the presence of glycine. In these experiments, we performed morphological studies on hippocampal neurons that had been cultured for 2 weeks (DIV15), which is when spines are in the maturation process *in vitro*[27] (Fig. 7a). Without glycine, the spine length and spine head volume were not significantly different regardless of FILIP (Fig. 7b–d). In contrast, the spine length decreased in the presence of FILIP when glycine was applied (1.15 ± 0.82 μm, 1513 spines from 11 control cells/glycine (−); 1.14 ± 0.82 μm, 1438 spines from 11 control cells/glycine (+); 1.20 ± 0.73 μm, 1421 spines from 11 FILIP-expressing cells/glycine (−); 1.05 ± 0.71 μm, 1736 spines from 11 FILIP-expressing cells/glycine (+); Fig. 7c). Interestingly, the application of glycine resulted in an increase in the spine head volume, and the degree of this enlargement was enhanced by FILIP expression (0.144 ± 0.202 μm^3, 1245 spines from 11 control cells/glycine -; 0.195 ± 0.276 μm^3, 1241 spines from 11 control cells/glycine +; 0.161 ± 0.193 μm^3, 1207 spines from 11 FILIP-expressing cells/glycine + and 0.233 ± 0.300 μm^3, 1451 spines from 11 FILIP-expressing cells/glycine +; Fig. 7d). In addition, we studied the effects of blebbistatin on spine length in the presence of glycine. A similar decrease in spine length was observed by the blebbistatin application as by FILIP (1.19 ± 0.90 μm, 396 spines with blebbistatin in the absence of glycine; 0.97 ± 0.87 μm, 305 spines with blebbistatin in the presence of glycine; 1.07 ± 0.81 μm, 555 spines with vehicle only in the absence of glycine; 1.15 ± 0.91 μm, 543 spines with vehicle only in the presence of glycine; Fig. 7e).

We further investigated how FILIP influences the intracellular distribution of NMDA receptors, especially the NR1 (NR1) and NR2A (NR2A) subunits. We counted the numbers of NR1- and NR2A-positive deposits in spines and divided them by the number of observed spines. We defined this value as the 'density of subunits in spines'. When FILIP was expressed, the densities of NR1- and NR2A-positive deposits were significantly lower (Fig. 7f, g; Fisher's exact test, two-tailed, NR1 p = 0.0211, NR2A p = 0.00009), suggesting that FILIP moderates NMDA receptor activity in the spine. We also investigated the proportion of NR2A-positive spines to all observed spines in the primary cultured piriform neurons in which the expression of FILIP was suppressed by inducible RNAi vectors. We observed a significant increase in NR2A-positive spines in FILIP-depleted piriform cortex neurons (control, 2.7% of 377 spines; *FILIP* knockdown, 5.6% of 444 spines; Fisher's exact test, two-tailed, p = 0.03807).

The response to NMDA is reduced in the piriform cortex of *FILIP*$^{-/-}$ mice. Because FILIP modified the distribution of NMDA receptors in the piriform cortex, we investigated whether responses to NMDA differed in the *FILIP*$^{-/-}$ mice compared with wild-type mice using calcium imaging techniques and a bath application of NMDA (see Supplemental Fig. S7 online). Neurons were less responsive to NMDA in the *FILIP*$^{-/-}$ mice compared with the wild-type littermates (Fig. 7h). Supplemental Fig. S8 depicts the FILIP effects on spines (see Supplemental Fig. S8 online).

The intracortical excitation propagation is abnormal in *FILIP*$^{-/-}$ mice. Because FILIP deletion resulted in an abnormal response to NMDA in the piriform cortex, we investigated whether FILIP influenced neuronal activity. Unlike other areas in the cortex, the visual cortex, where FILIP is expressed in layers II/III (Fig. 1g–i and Fig. 8a), receives strong and sole input from the thalamus, which allows us to investigate how neuronal activity propagates in the cortex by stimulating the thalamic input fibres. We stimulated the white matter of explants taken from the visual cortex so that axons from the lateral geniculate nucleus were activated and studied how neuronal activity was propagated using a voltage-sensitive dye[28]. The first excitation was observed in layer VI approximately 4.2 ms after stimulation (Fig. 8b). In the control, the excitation was subsequently propagated to the upper layers and spread laterally (horizontally) in layers II/III and layer VI (Fig. 8b). In the *FILIP*$^{-/-}$ mice, the degree of excitation in the upper cortical layers was lower than in the controls. In particular, the lateral propagation was reduced in layers II/III

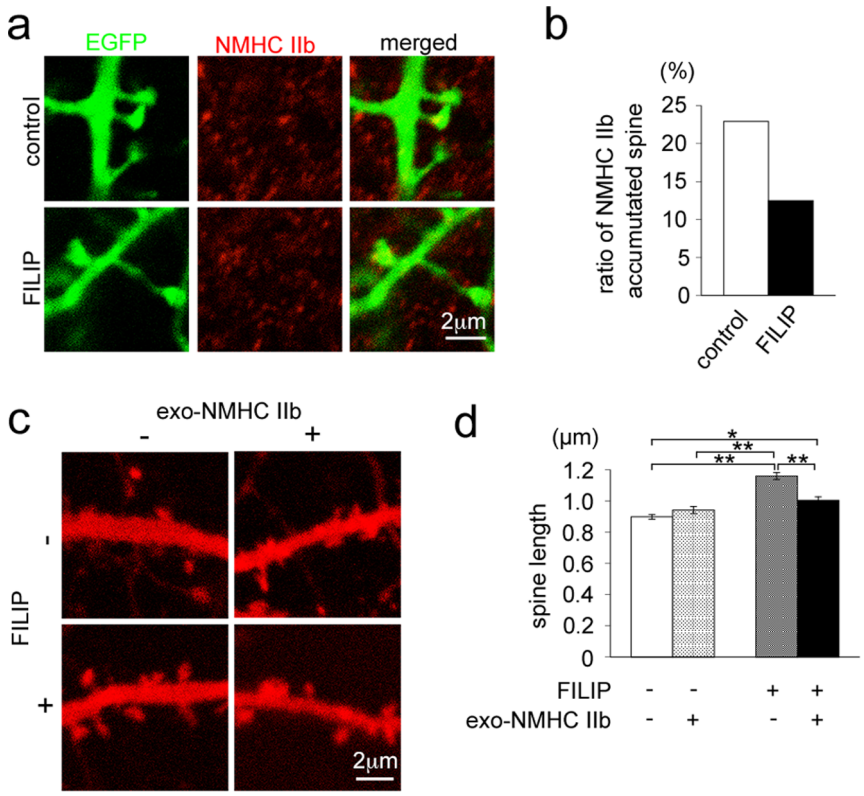

Figure 6 | Overexpression of NMHC IIb blocks the elongation of spines in the FILIP-expressing hippocampal neurons. (a) Endogenous NMHC IIb was less accumulated in the spine neck of the FILIP-expressing hippocampal neurons. (b) The summarised data of 816 spines (the control) and 649 spines (the FILIP-expressing neurons) are shown; $p < 0.00001$ (Fisher's exact test, two-tailed). (c) Exogenous NMHC IIb (exo-NMHC IIb) rescued the spine elongation due to FILIP overexpression in the hippocampal neurons. (d) The summarised data of 362 spines (FILIP-/exo-NMHC IIb–), 712 spines (FILIP-/exo-NMHC IIb+), 555 spines (FILIP+/exo-NMHC IIb–) and 828 spines (FILIP+/exo-NMHC IIb+) are shown. In each case, spines were selected from 5 neurons; * $p = 0.00386$, ** $p < 0.00001$ (Welch's *t*-test, two-tailed).

8.4 ms after the stimulation (Fig. 8b). Whereas the peak amplitude of excitation in layer VI was not significantly different between the control and the *FILIP*$^{-/-}$ mice, it was significantly different in layers II/III, where FILIP is principally expressed (Fig. 8a–c). The reduction in the horizontal propagation of excitation in layers II/III of the *FILIP*$^{-/-}$ mice persisted even when GABAergic transmission was inhibited by treatment with the $GABA_A$-receptor blocker bicuculline (Fig. 8d). We next investigated whether this phenomenon depended on the modification of myosin function by FILIP. We used blebbistatin to block myosin 2b activity and found that the excitation propagation was reduced in layers II/III of the visual cortex in wild-type mice, whereas that of *FILIP*$^{-/-}$ mice was not changed (Fig. 8e, f).

Discussion

We showed that FILIP bound to, and influenced the subcellular distribution of, myosin 2b. FILIP is likely to facilitate the degradation of NMHC IIb by modulating enzyme accessibility, because we observed that exogenous FILIP prevented NMHC IIb from binding to actin fibres, and it has been reported that the binding of myosin to actin fibres results in the protection of myosin from enzymatic digestion[29]. Although it is difficult to exclude the possibility that any compensatory activity of the *FILIP* knockout is responsible for an increase of myosin 2b, we observed an increase in the amount of NMHC IIb in *FILIP*$^{-/-}$ mice. We previously reported that FILIP enhances filamin A degradation[8]. Therefore, FILIP is likely to be a meta-regulator that orchestrates the activities of the major actin-binding proteins filamin A and myosin 2b.

We showed that FILIP deletion leads to a shorter spine length in the piriform cortex and that exogenous FILIP results in an elongated spine length in well-developed hippocampal neurons. These results indicate that FILIP, which is expressed in a region-specific manner, is a key molecule that confers unique regional spine characteristics.

The NR1, NR2A, and NR2B subunits of the NMDA receptor bind to the myosin regulatory light chain, which is one component of myosin 2b. It has been demonstrated that such binding influences the function of NMDA receptors and the intracellular trafficking of these subunits[30,31]. As FILIP bound to the heavy chain of myosin 2b and altered its distribution, it is possible that the distribution of NMDA receptor is also altered from the synaptic area to other regions, for example dendritic shafts. Furthermore, as FILIP accelerates the degradation of filamin A through calpain activity[8], the cleavage of NR2A receptor by the activated calpain may have resulted in the alteration of its distribution from the synaptic to extrasynaptic area[32]. We presumed that this alteration of localisation is the cause of the decrease of NR1 and NR2A signals in the spines of FILIP expressing neurons. While it is not completely clear how extrasynaptically localised NMDA receptors influence the neurons[32], it is possible that they are responsible for the high responses to glycine in FILIP expressing hippocampal neurons. Interestingly, at DIV15, when spine lengths are becoming shorter and the spine head wider[27], FILIP did not exert any significant influence on the spine morphology of hippocampal neurons without glycine. Because the maturation of cultured hippocampal neurons progresses greatly in the 2–3 weeks after the initiation of culture[27], our data suggest that FILIP did not influence the developmental changes of spine morphology in any apparent way.

It has been demonstrated that myosin 2 activity is required for NMDA receptor-dependent synaptic plasticity and for LTP-related dendritic spine actin polymerisation[6]. It is possible that FILIP con-

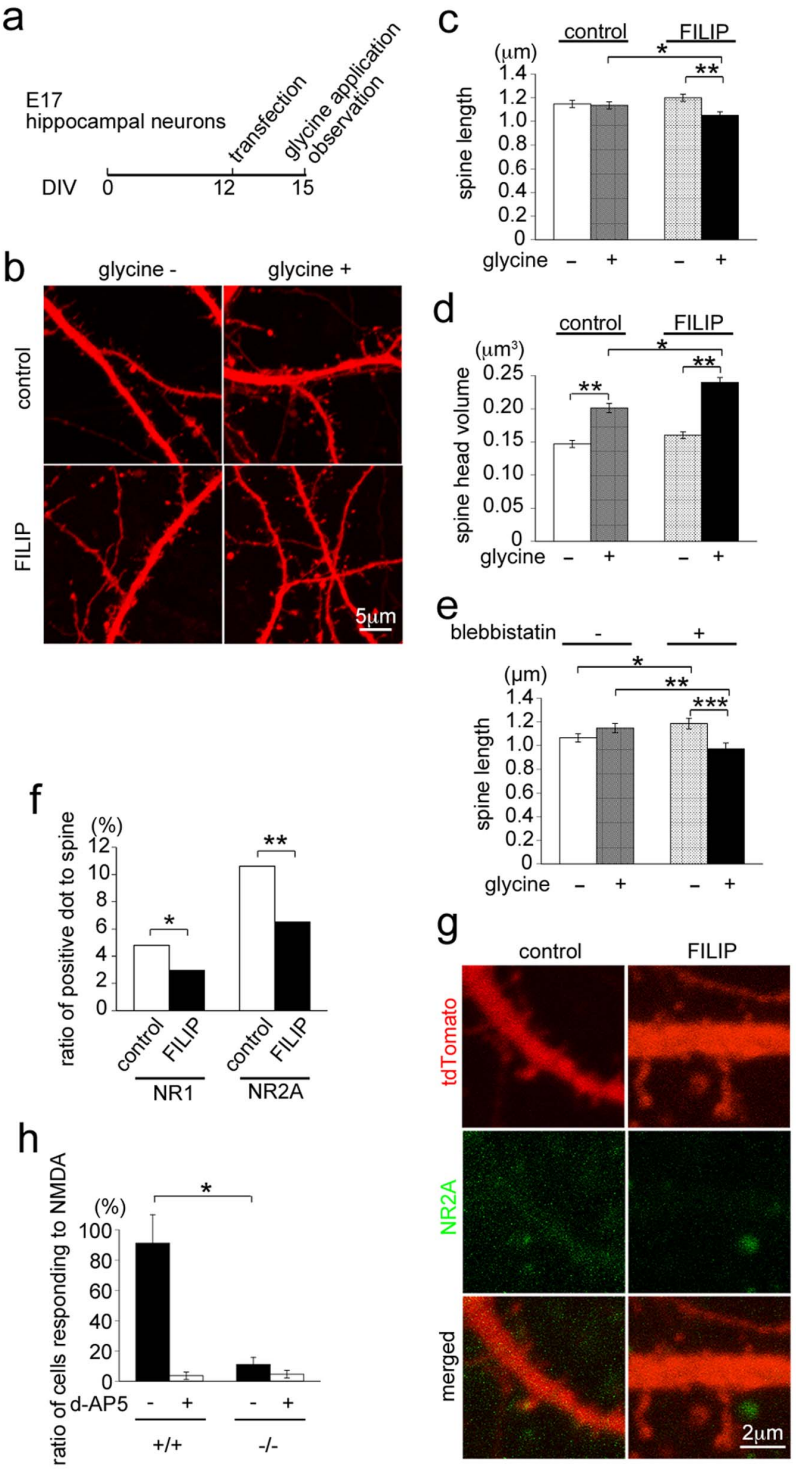

Figure 7 | FILIP influences the morphological changes of spines due to the glycine treatment. (a) The transfection and observation schedule are indicated. (b) The mean spine length of FILIP-expressing cells in the presence of glycine (glycine +) was significantly shorter than that of control cells, and the mean spine head volume of FILIP-expressing cells in the presence of glycine was significantly larger than that of control cells. (c) The mean spine lengths are shown. The mean spine length of FILIP-expressing cells in the presence of glycine was significantly shorter than that of control cells. * $p = 0.00237$, ** $p < 0.00001$ (Welch's *t*-test, two-tailed); error bars, s.e.m. (d) The mean spine head volumes are shown. The mean spine head volume of FILIP-expressing cells in the presence of glycine was significantly larger than that of control cells. * $p = 0.00071$, ** $p < 0.00001$ (Welch's *t*-test, two-tailed); error bars, s.e.m. (e) Blebbistatin influenced spine length in the presence of glycine. The mean spine lengths are shown. * $p = 0.03537$, ** $p = 0.00574$, *** $p = 0.00158$ (Welch's *t*-test, two-tailed); error bars, s.e.m. (f) The subcellular distribution of NMDA receptors was altered in FILIP-expressing cells. The data of NR1 staining obtained from 1231 spines from 9 control neurons and 1216 spines from 9 FILIP-expressing neurons are shown. The data of NR2A staining obtained from 1395 spines from 9 control neurons and 1462 spines from 9 FILIP-expressing neurons are shown; * $p = 0.03807$, ** $p = 0.00009$ (Fisher's exact test, two-tailed). (g) NR2A-positive dots in spines were decreased in FILIP-expressing cells. (h) NMDA was applied to the piriform cortex slices. The number of responding neurons was reduced in the *FILIP*$^{-/-}$ mice. The data obtained from 4 slices of 3 normal littermates and 8 sliced of 3 *FILIP*$^{-/-}$ mice are shown; *$p = 0.02041$ (Welch's *t*-test, two-tailed).

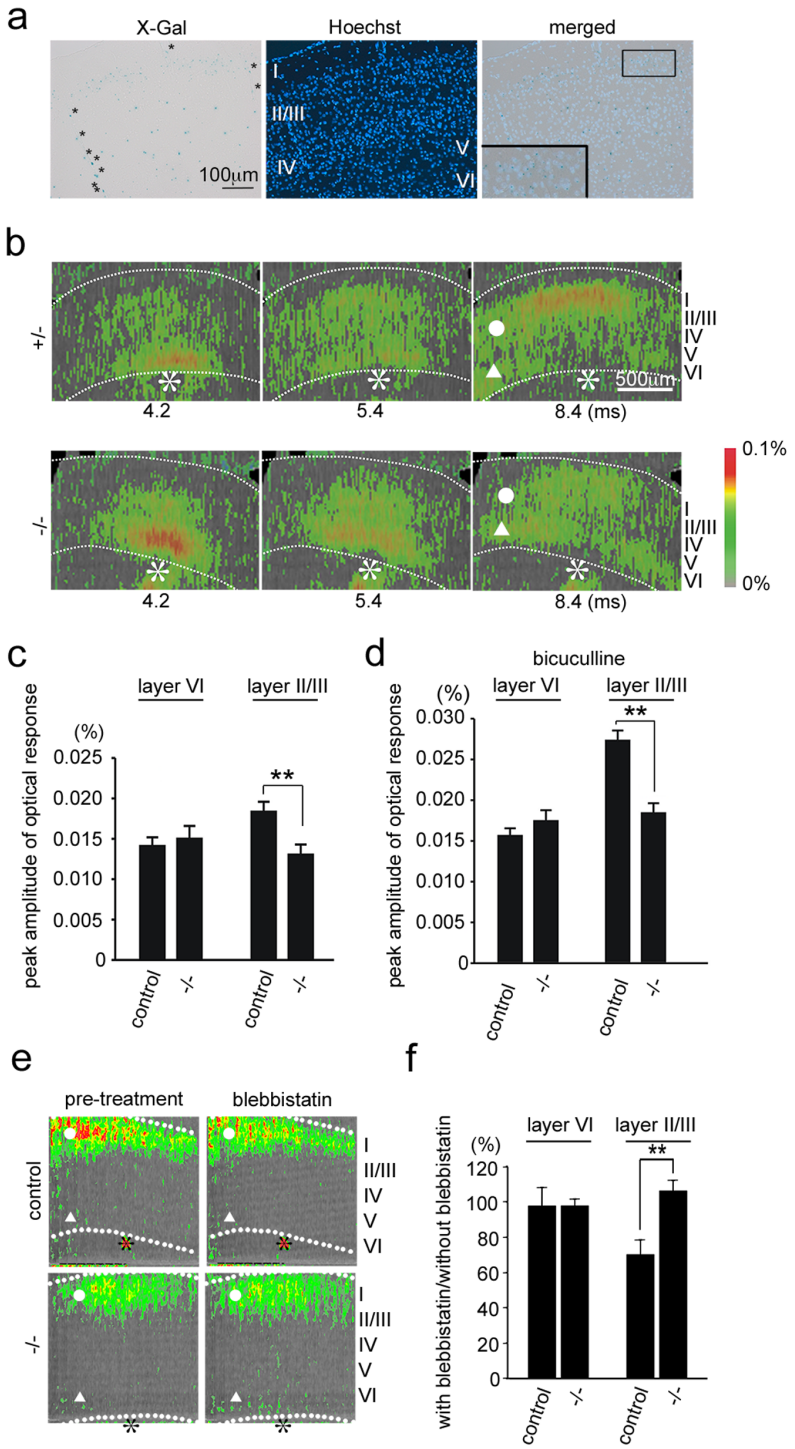

Figure 8 | The propagation of excitation in the visual cortex is impaired in *FILIP*$^{-/-}$ mice. (a) FILIP-positive cells in the visual cortex, detected using β-galactosidase activity, of the adult *FILIP*$^{-/-}$ mice are shown. Vascular endothelial cells exhibited strong endogenous β-galactosidase activity (*) that was not related to FILIP expression. The nuclei were visualised using Hoechst 33258. The cortical layers are indicated. In the right panel, a high-magnification image of the rectangle is shown in the inset. (b) Excitation in the visual cortex of the *FILIP*$^{-/-}$ mouse and *FILIP*$^{+/+}$ littermates was observed using a voltage-sensitive dye. The asterisks (*) indicate the sites of stimulation. The time (ms, millisecond) after the stimulus is shown. I–VI: cortical layers. The dotted lines indicate the pial surface of the cortex and the border between the white matter and layer VI. The colour bar shows the percentage change in light absorption. (c)(d) These graphs indicate the mean peak amplitudes of the optical responses obtained from 7 *FILIP*$^{-/-}$ mice and 5 control mice (*FILIP*$^{+/-}$ and *FILIP*$^{+/+}$ mice) 5 weeks after birth. (c) The peak amplitude of the optical responses obtained from the regions are indicated by the white circles (○) in layers II/III and the white triangles (Δ) in layer VI in the right panels of (a) during the observation. Error bars, s.e.m.; ** $p = 0.00249$ (Student's *t*-test, two-tailed). (d) The mean peak amplitude of the optical signals upon treatment with 2 μM bicuculline obtained from layer VI and layers II/III, as described above; ** $p = 0.00014$ (Student's *t*-test, two-tailed). (e) Blebbistatin treatment on a slice of the visual cortex resulted in the reduction of the propagation of excitation within layers II/III in the control mouse. (f) The ratios of peak amplitude of the optical signals with blebbistatin to without blebbistatin obtained from the regions are indicated by the white circles (○) in layers II/III and the white triangles (Δ) in layer VI in the right panels of (e) are shown. The data were obtained from 4 control slices and 6 *FILIP*$^{-/-}$ slices. Error bars, s.e.m.; ** $p = 0.00742$ (Student's *t*-test, two-tailed).

tributes to regional spine characteristics in learning[11,13,33] through the modification of NMDA receptor and myosin 2b function, while our glycine treatment on the FILIP expressing hippocampal neurons resulted in the enlargement of spine head volume. While we administered our glycine treatment without AP5 preconditioning[26,34] to avoid the alteration of expression of NMDA receptors by AP5 on the spines[35], it may be that the glycine treatment did not fully mimic the *in vivo* condition, especially in the case of the our primary culture neurons. As we have previously discussed, FILIP showed no significant effects on the spine morphology of primary cultured hippocampal neurons at DIV15 without glycine treatment. This result indicated that the conditions of the primary culture neurons in our glycine treatment were somewhat different from those of piriform neurons *in vivo* at the adult stage. It is possible that the morphological changes of FILIP expressing hippocampal neurons could not mimic that of the piriform neurons in their response to learning due to the difference in the *in vivo* and *in vitro* conditions.

The results of our blebbistatin treatment on the cortex indicated that myosin 2b function represents the function of FILIP on the horizontal propagation of excitation in the upper layer. As myosin 2b in the growth cone of axons is involved in axon elongation[36] and the myosin 2b activity regulates axon branching[37], there is a possibility that alterations in the subcellular distribution of myosin 2b due to FILIP altered the intra-cortical circuit related to the horizontal propagation of excitation. Furthermore, the decrease of FILIP expressing cells in the upper layer of cortex is probably one of the causes of the decrease of horizontal propagation of excitation because β-galactosidase positive cells decreased in the cortex of *FILIP*$^{-/-}$ mice compared to *FILIP*$^{+/-}$ mice.

Methods

Method details are given in the Supplemental information online.

Animals. The mice were maintained in the animal room at the Division of Laboratory Animal Resources, University of Fukui and Hyogo College of Medicine. The day of birth was designated P0. All experiments were conducted in accordance with the Regulations for Animal Research at University of Fukui and the Regulations for Animal Experimentation in Hyogo College of Medicine. The Animal Research Committee, University of Fukui and the President of Hyogo College of Medicine under the review of the Hyogo College of Medicine Animal Experiment Committee approved the experiments.

Generation of *FILIP*-knockout mice. Conventional methods were used for the generation of *FILIP*-knockout mice.

Vector construction. The full-length rat *l-FILIP* cDNA was amplified using PCR and inserted into the pCAGGS vector[38], which contains 3 × FLAG sequences and IRES GFP (pCAGGS FILIP IRES GFP). The empty-vector control was the pCAGGS vector expressing IRES GFP (pCAGGS IRES GFP). Vectors that express a truncated form of FILIP were constructed using the KOD-plus-mutagenesis kit (TOYOBO CO., LTD, Tokyo, Japan). The full-length and various fragments of *NMHC IIb* were amplified using PCR and inserted into the pCMV VSV vector to produce fragments tagged with VSV-G under the *CMV* promoter. The shRNA vector for *NMHC IIb* and *NMHC IIb*-resistant vector were constructed. The conditional knockdown vector for *FILIP* was constructed using the Tol2 transposon-mediated technique[39]. The target nucleotide was bp 1433–1453 of the mouse FILIP cDNA (GenBank accession number: BC131965.1). The primers for the vector construction are shown in the Supplemental information online.

Northern blot analyses. Conventional protocols were used for northern blot analyses[40].

Histochemical detection of β-galactosidase and immunostaining. After fixation with 4% paraformaldehyde (PFA), the brains were cut into 30-μm sections with a cryostat. The sections were stained with X-gal staining solution (1 mg/ml X-gal, 2 mM $MgCl_2$, 5 mM $K_3Fe(CN)_6$, 5 mM $K_4Fe(CN)_6$, 0.01% NP-40) at 37°C for 40–48 hr. For immunohistochemical analyses, the sections were incubated with antibody dilution solution for 30 min and incubated overnight at 4°C with the antibody dilution buffer containing appropriate concentration of antisera. The signals were visualised with Alexa Fluor 568-conjugated anti mouse IgG or Alexa Fluor 488-conjugated anti mouse IgG (Life Technologies Corporation, Grand Island, NY).

Golgi staining method. The FD Rapid GolgiStain kit (FD Neurotechnologies, Inc., Columbia, MD) was used for Golgi-Cox staining according to the manufacturer's protocol. The spine morphology in piriform layer II neurons was classified according to Harris's report[41].

The primary culture of neurons from the hippocampus and the piriform cortex. The hippocampus and piriform neurons at E17.5 were cultured on polyethyleneimine-coated coverslips with growth medium (neurobasal medium; Life Technologies Corporation) containing MACS Supplement B27 PLUS (Miltenyi Biotec GmbH, Bergisch Gladbach, Germany) and l-glutamine). For the analysis of spine morphology, the vectors were transfected using Lipofectamine 2000 (Life Technologies Corporation) at DIV17 or 18. To calculate the spine head volume and length, Z-stacked images were captured using a confocal microscope (LSM 5 Pascal, Carl Zeiss MicroImaging, GmbH, Jena, Germany) at DIV21. The spine head width and spine head length of the mushroom- or thin-type spines were measured using the ImageJ image analysis program (NIH, Bethesda, MD)[42]. Spine head volume was calculated according to the method of Knafo[13]. To treat cells with glycine, the vectors were transfected as described above at DIV12. At DIV15, the cells were incubated with 200 μM glycine-containing HEPES-buffered balanced salt solution (HEPES-BSS) supplemented with 0.5 μM tetrodotoxin, 1 μM strychnine and 20 μM bicuculline for 10 min following incubation with normal HEPES-BSS for 20 min. To be treated with 10 μM blebbistatin during the glycine treatment, the cells were preincubated with growth medium containing 10 μM blebbistatin for 30 min; then, the cells were treated with glycine as described above, with the exception of using HEPES-BSS supplemented with 10 μM blebbistatin. NMDA receptors were visualised using a polyclonal anti-NR1 antibody (Sigma-Aldrich Co. LLC, St. Louis, MO) or a polyclonal anti-NMDAR2A antibody (EMD Millipore Corporation, Billerica, MA) followed by Alexa Fluor 633-conjugated anti-rabbit IgG (Life Technologies Corporation). pCAGGS-tdTomato, pT2K-CAGGS-rtTAM2, pT2K-TBI-shRNAmir and pCAGGS-T2TP (Tol2 transposase) were transfected at a ratio of 1 : 4 : 2 : 4 using Lipofectamine 2000 at DIV16. The culture media were changed to doxycycline-containing media (1 μg/ml) at DIV17; the cells were observed at DIV21.

Immunoprecipitation. COS-7 cells that had been cultured in a 6-cm dish were lysed in 400 μl of ice-cold lysis buffer 24 hr after transfection with the plasmid vectors. Pre-cleared lysates were incubated with antibody-bound Protein G Dynabeads (Life Technologies Corporation) at 4°C for 3 hr. After the Dynabeads were rinsed three times in lysis buffer, the immunoprecipitated proteins were eluted in SDS sample buffer. Details are provided in the Supplemental information online.

Western blot analyses and anti-FILIP antisera. The cortices of the ICR mouse brains and hearts were homogenised in lysis buffer. The insoluble materials were removed through centrifugation. The protein concentration was measured using protein assay CBB solution (Nacalai Tesque, Inc., Kyoto, Japan). Protein lysates (5 μg) or immunoprecipitation products were separated through SDS-PAGE and transferred onto polyvinylidene difluoride membranes (EMD Millipore Corporation). After the membranes were blocked, they were incubated with primary antibodies followed by secondary antibodies coupled to HRP (1 : 2,000; BD Biosciences, Franklin Lakes, NJ). The peroxidase activity was detected using enhanced chemiluminescence. The blot densities were quantified using the ImageJ program. Anti-FILIP antisera were raised against a recombinant peptide of rat FILIP (ESQEMPMGRTILK) in rabbit.

***In utero* electroporation gene transfer of the inducible FILIP knockdown vector.** We performed in utero electroporation-mediated gene transfer as previously reported[39]. pCAGGS-tdTomato, pT2K-CAGGS-rtTAM2, pT2K-TBI-shRNAmir and pCAGGS-T2TP (Tol2 transposase) were transfected at a ratio of 1 : 10 : 5 : 10 into the embryonic brains of ICR mice at E14.5. At P21 to P28, the delivered pups were administered doxycycline via the drinking water (the final concentration was 2 mg/ml + 5% sucrose). The brains were dissected out at P28 and cut coronally into 100-μm slices with a Vibratome (DOSAKA EM Co., LTD., Kyoto, Japan).

Preparation for optical recording. We performed optical recording with some modifications from the previous reports[43,44]. For optical imaging of gross neuronal excitation, the slices (400-μm thick) were prepared from the visual cortices of *FILIP*$^{-/-}$ and their *FILIP*$^{+/+}$ or *FILIP*$^{+/-}$ littermates at one month of age. The slices were stained in a bath filled with RH-482 (0.1 mg/ml; 20 min). After completing the optical recordings under perfusion with Ringer's solution, the slice was perfused with Ringer's solution containing 2 μM bicuculline for 30 min. The optical recording in the presence of bicuculline was then performed.

Optical recording. The light absorption change at 700 ± 32 nm was recorded using an imaging system (Deltaron 1700; Fujifilm Corporation, Tokyo, Japan) with 128 × 128 pixel photo sensors at a frame rate of 0.6 ms. Starting at 10 ms before each stimulus, the image sensor took 128 consecutive frames at a sampling interval of 0.6 ms. A reference frame, which was taken immediately before each series of 128 frames, was subtracted from the subsequent 128 frames. An electric pulse was given to the white matter. The ratio image was then calculated by dividing the image data by the reference frame.

Ca^{2+} imaging. We performed Ca^{2+} imaging with some modifications from the previous report[44]. The brains were removed and transferred to an ice-cold aerated solution (95% O_2 and 5% CO_2) containing (in mM) 120 choline chloride, 2.4 KCl, 26 $NaHCO_3$, 1.2 NaH_2PO_4, 0.5 $CaCl_2$, 7 $MgCl_2$, 1.2 ascorbic acid and 15 glucose.

Coronal slices (300-μm thick) containing the piriform cortex were prepared using a vibrating microtome. Each slice was loaded for 45 min at room temperature with 10 μM Fluo-4/AM (Life Technologies Corporation) in the presence of 0.01% Pluronic F-127 (Life Technologies Corporation). The slices were then washed thoroughly with Ringer's solution and set in a chamber (0.2 mL) on an upright microscope (BX51WI; Olympus, Tokyo, Japan). Each slice was perfused with Ringer's solution containing (in mM) 127 NaCl, 2 KCl, 1.2 KH_2PO_4, 1.3 $MgSO_4$, 2.4 $CaCl_2$, 26 $NaHCO_3$ and 10 glucose (oxygenated with 95% O_2 and 5% CO_2) at room temperature (25 ± 2°C). The confocal images of fluo-4 fluorescence were captured in a 0.4-mm^2 area of the piriform cortex at a sampling interval of 500 ms using a CSU10 Nipkow spinning-disk confocal microscope (Yokogawa Electric, Tokyo, Japan) equipped with an EM CCD camera (iXON EM; Andor Technology Ltd., Belfast, Northern Ireland, UK). Fluo-4 fluorescence at 518 nm was excited by light at 488 nm from a semiconductor laser. NMDA (50 μM) or a high-K^+ solution were puff-applied for 10 s beginning at 10 s after the start of recording. The high-K^+ solution was identical to the Ringer's solution except for (in mM) in addition of 76 NaCl and 50 KCl.

Statistical analyses. To analyse the statistical significance of means, we used an unpaired two-tailed Student *t*-test when two samples had equal variances and Welch's *t*-test when two samples had unequal variances. To analyse statistical significance of the spine head volume, we used the Wilcoxon rank sum test or Welch's *t*-test. To analyse statistical significance of ratio, we used Fisher's exact test.

1. Le Clainche, C. & Carlier, M. F. Regulation of actin assembly associated with protrusion and adhesion in cell migration. *Physiol. Rev.* **88**, 489–513 (2008).
2. Honkura, N., Matsuzaki, M., Noguchi, J., Ellis-Davies, G. C. & Kasai, H. The subspine organization of actin fibers regulates the structure and plasticity of dendritic spines. *Neuron* **57**, 719–729 (2008).
3. Hotulainen, P. & Hoogenraad, C. C. Actin in dendritic spines: connecting dynamics to function. *J. Cell Biol.* **189**, 619–629 (2010).
4. Ryu, J., Liu, L., Wong, T. P., Wu, D. C. *et al.* A critical role for myosin IIb in dendritic spine morphology and synaptic function. *Neuron* **49**, 175–182 (2006).
5. Vicente-Manzanares, M., Ma, X., Adelstein, R. S. & Horwitz, A. R. Non-muscle myosin II takes centre stage in cell adhesion and migration. *Nat. Rev. Mol. Cell Biol.* **10**, 778–790 (2009).
6. Rex, C. S., Gavin, C. F., Rubio, M. D., Kramar, E. A. *et al.* Myosin IIb regulates actin dynamics during synaptic plasticity and memory formation. *Neuron* **67**, 603–617 (2010).
7. Hodges, J. L., Newell-Litwa, K., Asmussen, H., Vicente-Manzanares, M. & Horwitz, A. R. Myosin IIb activity and phosphorylation status determines dendritic spine and post-synaptic density morphology. *PLoS One* **6**, e24149 (2011).
8. Nagano, T., Yoneda, T., Hatanaka, Y., Kubota, C. *et al.* Filamin A-interacting protein (FILIP) regulates cortical cell migration out of the ventricular zone. *Nat. Cell Biol.* **4**, 495–501 (2002).
9. Fox, J. W., Lamperti, E. D., Ekşioğlu, Y. Z., Hong, S. E. *et al.* Mutations in filamin 1 prevent migration of cerebral cortical neurons in human periventricular heterotopia. *Neuron* **21**, 1315–1325 (1998).
10. Feng, Y. & Walsh, C. A. The many faces of filamin: a versatile molecular scaffold for cell motility and signalling. *Nat. Cell Biol.* **6**, 1034–1038 (2004).
11. Matsuzaki, M., Honkura, N., Ellis-Davies, G. C. & Kasai, H. Structural basis of long-term potentiation in single dendritic spines. *Nature* **429**, 761–766 (2004).
12. Matus, A. Actin-based plasticity in dendritic spines. *Science* **290**, 754–758 (2000).
13. Knafo, S., Libersat, F. & Barkai, E. Olfactory learning-induced morphological modifications in single dendritic spines of young rats. *Eur. J. Neurosci.* **21**, 2217–2226 (2005).
14. Mullen, R. J., Buck, C. R. & Smith, A. M. NeuN, a neuronal specific nuclear protein in vertebrates. *Development* **116**, 201–211 (1992).
15. Whittaker, S. G., Wroble, J. T., Silbernagel, S. M. & Faustman, E. M. Characterization of cytoskeletal and neuronal markers in micromass cultures of rat embryonic midbrain cells. *Cell Biol. Toxicol.* **9**, 359–375 (1993).
16. Molyneaux, B. J., Arlotta, P., Menezes, J. R. & Macklis, J. D. Neuronal subtype specification in the cerebral cortex. *Nat. Rev. Neurosci.* **8**, 427–437 (2007).
17. Fiala, J. C., Feinberg, M., Popov, V. & Harris, K. M. Synaptogenesis via dendritic filopodia in developing hippocampal area CA1. *J. Neurosci.* **18**, 8900–8911 (1998).
18. Holtmaat, A. J., Trachtenberg, J. T., Wilbrecht, L., Shepherd, G. M. *et al.* Transient and persistent dendritic spines in the neocortex in vivo. *Neuron* **45**, 279–291 (2005).
19. Noam, Y., Phan, L., McClelland, S., Manders, E. M. *et al.* Distinct regional and subcellular localization of the actin-binding protein filamin A in the mature rat brain. *J. Comp. Neurol.* **520**, 3013–3034 (2012).
20. Sellers, J. R. Myosins: a diverse superfamily. *Biochim. Biophys. Acta* **1496**, 3–22 (2000).
21. Pellegrin, S. & Mellor, H. Actin stress fibres. *J. Cell Sci.* **120**, 3491–3499 (2007).
22. Goeckeler, Z. M., Bridgman, P. C. & Wysolmerski, R. B. Nonmuscle myosin II is responsible for maintaining endothelial cell basal tone and stress fiber integrity. *Am. J. Physiol. Cell Physiol.* **295**, C994–1006 (2008).
23. Kovács, M., Tóth, J., Hetényi, C., Málnási-Csizmadia, A. & Sellers, J. R. Mechanism of blebbistatin inhibition of myosin II. *J. Biol. Chem.* **279**, 35557–35563 (2004).
24. Korobova, F. & Svitkina, T. Molecular architecture of synaptic actin cytoskeleton in hippocampal neurons reveals a mechanism of dendritic spine morphogenesis. *Mol. Biol. Cell* **21**, 165–176 (2010).
25. Thomson, A. M., Walker, V. E. & Flynn, D. M. Glycine enhances NMDA-receptor mediated synaptic potentials in neocortical slices. *Nature* **338**, 422–424 (1989).
26. Lu, W., Man, H., Ju, W., Trimble, W. S. *et al.* Activation of synaptic NMDA receptors induces membrane insertion of new AMPA receptors and LTP in cultured hippocampal neurons. *Neuron* **29**, 243–254 (2001).
27. Papa, M., Bundman, M. C., Greenberger, V. & Segal, M. Morphological analysis of dendritic spine development in primary cultures of hippocampal neurons. *J. Neurosci.* **15**, 1–11 (1995).
28. Tanifuji, M., Sugiyama, T. & Murase, K. Horizontal Propagation of Excitation in Rat Visual Cortical Slices Revealed by Optical Imaging. *Science* **266**, 1057–1059 (1994).
29. Mornet, D., Bertrand, R. U., Pantel, P., Audemard, E. & Kassab, R. Proteolytic approach to structure and function of actin recognition site in myosin heads. *Biochemistry* **20**, 2110–2120 (1981).
30. Amparan, D., Avram, D., Thomas, C. G., Lindahl, M. G. *et al.* Direct interaction of myosin regulatory light chain with the NMDA receptor. *J. Neurochem.* **92**, 349–361 (2005).
31. Bajaj, G., Zhang, Y., Schimerlik, M. I., Hau, A. M. *et al.* N-methyl-D-aspartate receptor subunits are non-myosin targets of myosin regulatory light chain. *J. Biol. Chem.* **284**, 1252–1266 (2009).
32. Gladding, C. M. & Raymond, L. A. Mechanisms underlying NMDA receptor synaptic/extrasynaptic distribution and function. *Mol. Cell. Neurosci.* **48**, 308–320 (2011).
33. Van Harreveld, A. & Fifkova, E. Swelling of dendritic spines in the fascia dentata after stimulation of the perforant fibers as a mechanism of post-tetanic potentiation. *Exp. Neurol.* **49**, 736–749 (1975).
34. Fortin, D. A., Davare, M. A., Srivastava, T., Brady, J. D. *et al.* Long-term potentiation-dependent spine enlargement requires synaptic Ca2+-permeable AMPA receptors recruited by CaM-kinase I. *J. Neurosci.* **30**, 11565–11575 (2010).
35. Molnár, E. Long-term potentiation in cultured hippocampal neurons. *Semin. Cell Dev. Biol.* **22**, 506–513 (2011).
36. Yu, P., Santiago, L. Y., Katagiri, Y. & Geller, H. M. Myosin II activity regulates neurite outgrowth and guidance in response to chondroitin sulfate proteoglycans. *J. Neurochem.* **120**, 1117–1128 (2012).
37. Ohnami, S., Endo, M., Hirai, S., Uesaka, N. *et al.* Role of RhoA in activity-dependent cortical axon branching. *J. Neurosci.* **28**, 9117–9121 (2008).
38. Niwa, H., Yamamura, K. & Miyazaki, J. Efficient selection for high-expression transfectants with a novel eukaryotic vector. *Gene* **108**, 193–199 (1991).
39. Iguchi, T., Yagi, H., Wang, C. C. & Sato, M. A tightly controlled conditional knockdown system using the tol2 transposon-mediated technique. *PLoS One* **7**, e33380 (2012).
40. Sambrook, J. & Russell, D. Molecular Cloning: A Laboratory Manual (CSHL Press, NY, USA, 2001).
41. Harris, K. M., Jensen, F. E. & Tsao, B. Three-dimensional structure of dendritic spines and synapses in rat hippocampus (CA1) at postnatal day 15 and adult ages: implications for the maturation of synaptic physiology and long-term potentiation. *J. Neurosci.* **12**, 2685–2705 (1992).
42. Collins, T. J. ImageJ for microscopy. *Biotechniques* **43**, 25–30 (2007).
43. Kiritoshi, T., Ikeda, H. & Murase, K. Long-term potentiation of neuronal excitation in the central nucleus of the rat amygdala revealed by imaging with a voltage-sensitive dye. *Brain Res.* **1349**, 32–40 (2010).
44. Ikeda, H., Kiritoshi, T. & Murase, K. Contribution of microglia and astrocytes to the central sensitization, inflammatory and neuropathic pain in the juvenile rat. *Mol. pain* **8**, 43 (2012).

Acknowledgments

We are grateful to Dr. M. Takahashi (Hokkaido Univ) for the myosin 2b cDNA, to Dr. Y. Yoshimura (NIPS), Dr. Y. Ishikawa (NAIST) and Dr. Y. Oka (Osaka Univ) for helpful discussions, to M. Murota, H. Yoshikawa, S. Kanae, C.C. Wang and H. Miyagoshi for technical assistance and to T. Taniguchi for secretarial assistance. This work was supported in part by the Competitive Allocation Fund and the Multidisciplinary Program for Elucidating the Brain Development from Molecules to Social behaviour (Fukui Brain Project) of University of Fukui, Grant-in-Aid for Researchers (Hyogo College of Medicine, 2013) and a Grant-in-Aid for Scientific Research and the Strategic Research Program for Brain Sciences "Integrated research on neuropsychiatric disorders" from the Ministry of Education, Culture, Sports, Science and Technology (MEXT) of Japan.

Author contributions

H.Y. carried out most of the experiments and analysed the data. M.S. initially conceived the project and directed the research. T.N., S.M. and M.O. generated the FILIP knockout mice. M.K. prepared the samples for histological analyses. R.M.T. and T.I. prepared plasmid vectors. M.-J.X. and K.K. prepared and manipulated the primary culture of hippocampal neurons. H.I and K.M carried out the optical recording and the Ca^{2+} imaging. M.S. wrote the manuscript together with H.Y. and all authors contributed to the final version.

Additional information

Supplementary information accompanies this paper at http://www.nature.com/scientificreports

Competing financial interests: The authors declare no competing financial interests.

How to cite this article: Yagi, H. *et al.* Filamin A-interacting protein (FILIP) is a region-specific modulator of myosin 2b and controls spine morphology and NMDA receptor accumulation. *Sci. Rep.* **4**, 6353; DOI:10.1038/srep06353 (2014).